scientific reports

Check for updates

OPEN

Development and validation of a visual nomogram for predicting clinically significant prostate cancer in negative mpMRI using ^{68}Ga-PSMA PET/CT

Wei Hu[1,2], ShiKuan Guo[3], XiangLiang Meng[1], FuLi Wang[1], ShuaiJun Ma[1], Chao Zhang[1], JingYi Wang[4], Lei Yuan[5], LongLong Zhang[1], YuMing Jing[1], Jian Chen[6], HaoZhong Hou[1], Yang Wang[5], KeYing Zhang[1], Yu Li[1,7], Fei Kang[4], DongHui Han[1], HongQian Guo[8], JingLiang Zhang[1], Jing Ren[5] & WeiJun Qin[1]✉

Multi-parametric magnetic resonance imaging (mpMRI) is a valuable medical technology for detecting clinically significant prostate cancer (csPCa). The diagnostic accuracy of mpMRI for csPCa in negative mpMRI (PI-RADS 1–2) remains suboptimal, underscoring the need for improvements for csPCa. This study aimed to build a visual predictive nomogram for early detection of csPCa in negative mpMRI. We retrospectively reviewed 303 men from our institution who simultaneously underwent ^{68}Ga-PSMA-11 PET/CT and mpMRI before a biopsy between March 2020 and July 2022 and 130 men from the outside institution (Nanjing Drum Tower Hospital) as external validation between September 2021 and June 2022. The enrolled patients in our institution were randomly divided into the training set (n = 212) and the internal validation set (n = 91). Multivariate logistic regression was performed to identify independent predictors and establish a nomogram using SUVmax of ^{68}Ga-PSMA-11 PET/CT and prostatic specific antigen density (PSAD) to predict the occurrence of csPCa in negative mpMRI. Multivariate logistic regression demonstrated that SUVmax (odds ratio [OR] 5.296, 95% confidence interval [CI] 1.691–23.972), and PSAD (OR 4.867, 95%CI 2.389–10.901) were independent predictors for csPCa in negative mpMRI. The area under the curve (AUC) of the nomogram was 0.819 (95%CI 0.729–0.890). Additionally, both the decision curve analysis (DCA) curve and the net reclassification improvement (NRI) showed significant improvements for csPCa in our model. External validation validated the reliability of the prediction nomogram. The visual interactive web risk calculator PI-RADS/SUVmax/PSAD model (PSP Model, www.cspca.online) based on the nomogram allows us to assess the risk of having csPCa. The nomogram based on preoperative examination was developed to predict csPCa in negative mpMRI and help reduce unnecessary biopsies. The visual PSP Model is an effective and accurate tool for urologists to use in the early prediction and timely management of csPCa.

Keywords Prostate cancer, ^{68}Ga-PSMA PET/CT, MpMRI, Nomogram, Diagnosis

Abbreviations

[1]Department of Urology, Xijing Hospital, Fourth Military Medical University, No.127, Changle West Road, Xi'an 710032, Shaanxi, China. [2]Department of Urology, No.967th Hospital of Joint Logistic Support Force of PLA, Dalian, Liaoning, China. [3]Department of Urology, No.988th Hospital of Joint Logistic Support Force of PLA, Zhengzhou, Henan, China. [4]Department of Nuclear Medicine, Xijing Hospital, Fourth Military Medical University, Xi'an, China. [5]Radiology, Xijing Hospital, Fourth Military Medical University, Xi'an, China. [6]Department of Urology, Northwest University First Hospital, Xi'an, China. [7]Department of Urology, Institute of Surgery Research, Daping Hospital, Army Medical University, Chongqing, China. [8]Department of Urology, Institute of Urology, Nanjing Drum Tower Hospital, Affiliated Hospital of Nanjing University Medical School, Nanjing University, Nanjing, China. ✉email: qinwj_fmmu@163.com

^{68}Ga-PSMA PET/CT	^{68}Ga Prostate-specific membrane antigen positron emission tomography/computerized tomography
ADC	Apparent diffusion coefficient
AUC	Area under the curve
C-Index	Concordance index
csPCa	Clinically significant prostate cancer
DCA	Decision curve analysis
DCE	Dynamic contrast-enhanced
DRE	Digital rectal examination
DWI	Diffusion-weighted imaging
EAU	European association of urology
IDI	Integrated discrimination improvement
IPW	Inverse probability weighting
ISUP	International society of urological pathology
mpMRI	Multi-parametric magnetic resonance imaging
NPV	Negative predictive value
NRI	Net reclassification improvement
PI-RADS	Prostate imaging-reporting and data system
PPV	Positive predictive value
PSA	Prostatic specific antigen
PSAD	PSA density
PV	Prostate volume
ROC	Receiver operating characteristic
SBx	Systematic biopsy
T2WI	T2-Weighted imaging
TBx	Target biopsy
TRUS	Transrectal ultrasound-guided

According to GLOBOCAN estimates of cancer data[1]the incidence and mortality rates of prostate cancer have been steadily increasing, making it a significant disease affecting the quality of life and adding to the economic burden on families. Transrectal ultrasound-guided (TRUS) biopsy is usually performed in men with elevated serum prostatic specific antigen (PSA) and an abnormal digital rectal examination (DRE)[2]. When the diameter of the lesion was small (< 0.5 cm), the detection rate of mpMRI decreased significantly[3]. A positive mpMRI with an apparent tumor lesion would improve the definition of the suspicious area and enable a targeted biopsy to be performed. Conversely, a negative mpMRI without an apparent lesion might allow urologists to hesitate and patients to defer biopsy. According to statistics, approximately 1 in 10 latter may have csPCa lesions (Gleason score ≥ 3 + 4) in negative or nonsuspicious mpMRI[4].

However, there is no consensus on whether patients with suspected prostate cancer and negative mpMRI should undergo a biopsy. The European Association of Urology (EAU) guidelines on prostate cancer suggest individualized follow-up when mpMRI is negative[2]. However, deferring biopsy solely on the basis of a negative mpMRI carries the risk of missing csPCa. It has been reported that 3.8–15.6% of patients with negative mpMRI were subsequently diagnosed with csPCa by biopsy[5,6]. How to spare patients with negative mpMRI from prostate biopsy while avoiding leakage is the focus of clinical studies.

^{68}Ga prostate-specific membrane antigen positron emission tomography/computerized tomography (^{68}Ga-PSMA PET/CT) is a novel molecular imaging technique that can help diagnose prostate cancer and assess tumor burden. Increasing evidence has indicated the unique advantages of ^{68}Ga-PSMA PET/CT in detecting primary prostate cancer[7]. The detection of node metastases is better than that of whole-body MRI in primary staging of PCa[8]. Previous studies have shown that PSMA PET/CT has a higher positive predictive value (PPV) and negative predictive value (NPV) than mpMRI in the diagnosis of the primary tumor (85% vs. 81% and 88% vs. 76%)[9]. In postoperative monitoring, enlarged nodules with higher SUVmax contributed significantly to PSA increase, suggesting the unique value of PSMA PET/TC in the localization of biochemical recurrence[10]. Due to their differences in imaging principles and anatomical precision, both methods might miss tumors, but they also showed complementary roles. Combining these two techniques can reduce the percentage of missed lesions and yield a detection rate of 99.5%[11].

This study aimed to evaluate the added diagnostic value of the ^{68}Ga-PSMA PET/CT to negative mpMRI in detecting csPCa and build a nomogram to improve the diagnostic accuracy of csPCa in negative mpMRI. The interactive web risk calculator based on the nomogram can conveniently provide clinicians with an accurate and effective tool for the early risk prediction and timely management of csPCa.

Materials and methods

Patients

In Xijing Hospital, we retrospectively reviewed 797 patients with suspected prostate cancer who underwent both ^{68}Ga-PSMA PET/CT and mpMRI between March 2020 and July 2022, of which 70% of patients were divided into the training set ($n = 212$), and the rest were divided into the internal validation set ($n = 91$). In Nanjing Drum Tower Hospital, all of 130 eligible patients (negative mpMRI) from September 2021 to June 2022 were divided into the external validation set. The flowchart is shown in Figure S1. Finally, 433 men were enrolled for analysis. Ethical approval for this study was obtained from the local ethics committee. Due to the retrospective nature of the study, the Medical Ethics Committees of Xijing Hospital and Nanjing Drum Tower Hospital waived the need of obtaining informed consent.

Collection and evaluation of mpMRI images

All images were acquired with 3.0T MR scanners (GE 750, Siemens Magnetom Trio, and Philips Achieva) and 8-channel belly phased-control coils. The primary scanning sequences included axial T2-weighted imaging (T2WI), diffusion-weighted imaging (DWI) with high b value (b = 0, 1500 s/mm^2), apparent diffusion coefficient (ADC) mapping, and dynamic contrast-enhanced (DCE) images. The scanning parameters are shown in Table S1. Two genitourinary radiologists with 10 and 15 years of experience (W.Y. and R.J.) evaluated mpMRI according to Prostate Imaging-Reporting and Data System (PI-RADS) V2.1[12]. Any divergence will be resolved by consensus with a third radiologist (H.Y., 25 years' experience). We define negative mpMRI as PI-RADS 1–2 and positive as PI-RADS 3–5. Prostate volume (PV) was calculated from MRI.

Collection and evaluation of ^{68}Ga-PSMA PET/CT images

^{68}Ga-PSMA-11 PET/CT images were acquired with the Siemens Biograph 40 system (Germany) and United Imaging Healthcare 780 PET/CT scanner (China). ^{68}Ga-PSMA-11 was prepared according to a previously published protocol[13]. The scanning parameters are shown in Table S1. The ^{68}Ga-PSMA PET/CT images were reviewed by two experienced nuclear medicine specialists with 18 and 9 years of experience (F.K. and J.Y.W.). Any divergence will be resolved by consensus with a third radiologist (W.J., 30 years' experience). The SUVmax calculation of lesions is consistent with previous reports[13]. The PRIMARY score was evaluated according to the previous PRIMARY score study[14].

Pathologic evaluation

All patients underwent a standard transrectal ultrasound-guided 12-core systematic biopsy (SBx) and necessary additional target biopsy (TBx). Lesions were defined using the PI-RADS v2.1 system. MRI and transrectal ultrasound fusion targeted prostate biopsy were performed using cognitive targeting, and the biopsy was performed under real-time ultrasound guidance. Patients undergoing TBx had 2–3 cores taken per mpMRI-defined lesion. Two experienced pathologists scored the highest Gleason score on the biopsy specimens and International Society of Urological Pathology (ISUP) grade according to the standard[15]. Referring to previous research[16]the clinically significant disease was defined as having any Gleason ≥ 3 + 4 or ISUP ≥ 2 on histologic evaluation.

Development and assessment of the nomogram

Independent predictors ($P < 0.05$) were assessed by multivariate logistic regression and then recruited to develop the nomogram for predicting the occurrence of csPCa in negative mpMRI. After that, the prediction model was externally validated. The Hosmer-Lemeshow test was used to assess the model's goodness of fit. The receiver operating characteristic (ROC) curve, AUC, concordance index (C-index), and calibration curve were used to evaluate the predictive accuracy and conformity of the model. The DCA reflected the net benefit of the nomogram for patients. The NRI assessed the improvement in the predictive performance of the nomogram by quantifying the proportion of patients correctly reclassified into more appropriate risk categories.

Statistical analysis

Continuous variables were present as median (interquartile ranges), and the categorical variables were presented as frequencies (percentages). Univariate and multivariate logistic regression analyses were performed to identify predictors of csPCa. All statistical analysis was performed using SPSS 26.0 (IBM, Inc., Chicago, IL, USA) and R software, version 3.4.2 (R Foundation for Statistical Computing, Vienna, Austria). All reported P values were two-sided, and P value < 0.05 was considered statistically significant.

Results

Patient characteristics

The clinical characteristics of 433 enrolled men are presented in Table 1. PV and DRE did not display a statistical difference ($P > 0.05$) between the training set and the internal and external validation set.

Pathological results

The pathological results are detailed in Fig. 1 and Table S2. The prevalence of csPCa and any cancer was 103/433 (23.79%) and 207/433 (47.81%), respectively. There was no significant difference in the ratio of csPCa between institutions 1 and 2 (46.4% vs. 54.9%, $p = 0.233$). Among patients with PI-RADS 1–2 scores, only 5.94% underwent combined biopsy (SBx + TBx), where targeted biopsy is less commonly performed for patients with low PI-RADS scores and affected pathology results (22.22% vs. 18.95%, $p = 0.7577$).

Screening for predictive factors

The identified independent predictors of csPCa in patients with negative mpMRI by univariate logistic regression were shown in Table S3. LASSO regression was then applied to select the most significant predictors (Fig. 2). PSAD and SUVmax of ^{68}Ga-PSMA-11 PET/CT were identified as independent predictors and subsequently validated in the training, internal validation, and external validation sets (all $p < 0.05$, Table 2), forming the basis for constructing the final nomogram.

Risk prediction nomogram development

The logistic regression model was constructed based on the above two factors, after which these two clinical factors from the logistic regression model were integrated into the nomogram (C-index = 0.819) (Fig. 3). In addition, The Hosmer-Lemeshow test demonstrated that the model was a good fit ($P = 0.643$). We calculated the prediction probabilities for each sample using the model in external validation. By plotting the performance

Parameters	Overall	Institution 1		Institution 2	*p*-value
		Training Set	Internal Validation Set	External Validation Set	
Patients	433	212	91	130	—
Ages, years	68.0 (64.0,74.0)	68.0 (63.0,73.0)	67.0 (61.0,71.5)	68.0 (64.0,74.0)	< 0.001
PSA, ng/ml	9.65 (6.63, 15.02)	8.90 (6.23, 12.90)	10.30 (6.45, 18.39)	10.28 (7.35, 18.39)	0.014
PV, cm^3	50.62 (33.42, 67.27)	52.12 (34.57, 68.75)	44.29 (31.31, 65.87)	50.84 (31.84, 66.24)	0.208
PSAD, $ng/ml/cm^3$	0.19 (0.11, 0.36)	0.17 (0.11, 0.28)	0.21 (0.12, 0.49)	0.23 (0.14, 0.44)	0.001
SUVmax	5.60 (3.75, 8.20)	5.10 (3.70, 7.20)	5.60 (3.70, 8.70)	6.35 (4.08, 9.53)	0.027
PRIMARY score (%)					0.028
1	106 (24.48)	58 (27.36)	20 (21.98)	28 (21.54)	
2	143 (33.03)	74 (34.91)	35 (38.46)	34 (26.15)	
3	90 (20.79)	43 (20.28)	18 (19.78)	29 (22.31)	
4	56 (12.93)	25 (11.79)	7 (7.69)	24 (18.46)	
5	38 (8.78)	12 (5.66)	11 (12.09)	15 (11.54)	
DRE					0.719
Positive [n (%)]	333 (76.9)	164 (77.4)	72 (79.1)	97 (74.6)	
Negative [n (%)]	100 (23.1)	48 (22.6)	19 (20.9)	33 (25.4)	

Table 1. Clinical characteristics of patients in training, validation, and test set. PV, prostate volume; PSAD, PSA density; SUVmax, maximum standardized uptake value; DRE, digital rectal examination.

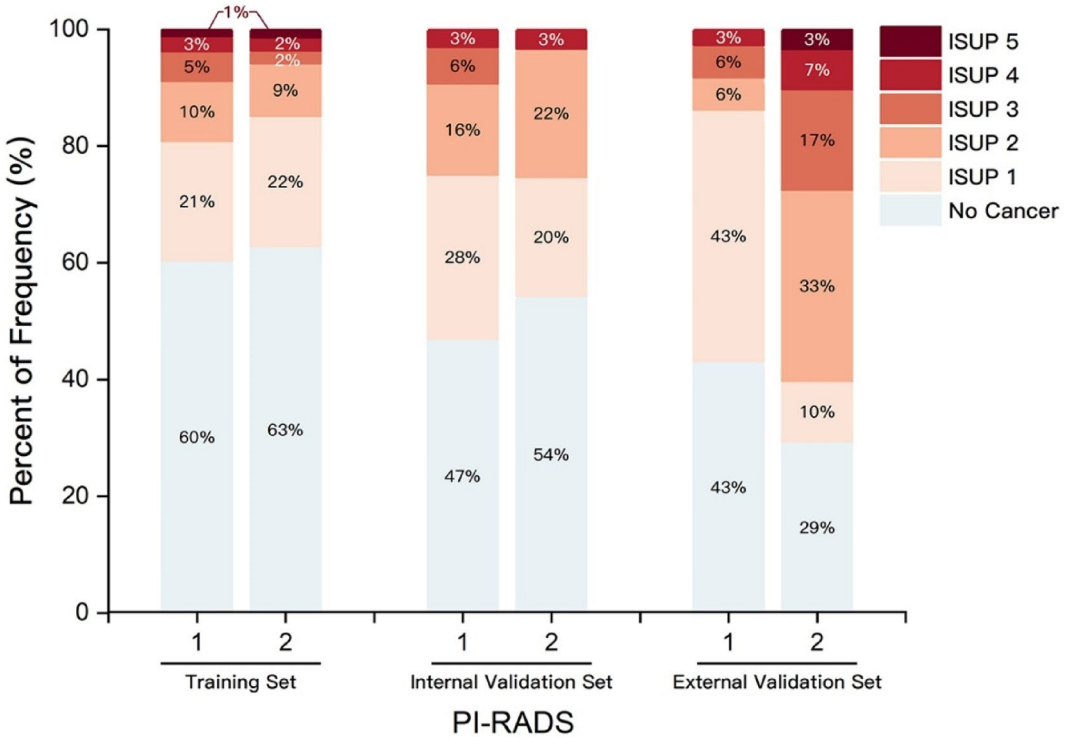

Fig. 1. Pathology results of patients with negative mpMRI.Bar chart showing the distribution of ISUP in PI-RADS 1-2 in training, internal, and external validation sets. Data were presented as percent of frequency.

metrics (sensitivity, specificity, PPV, and NPV) across different thresholds (Figure S2) and considering specific clinical requirements (e.g., reducing overdiagnosis or avoiding missed diagnoses), we identified 0.3 as the optimal clinical threshold. Compared with the cutoff value of 0.147 based on the maximum Youden Index in the training set, the net benefit at 0.3 is clinically significant in scenarios prioritizing the minimization of unnecessary interventions (Table S4).

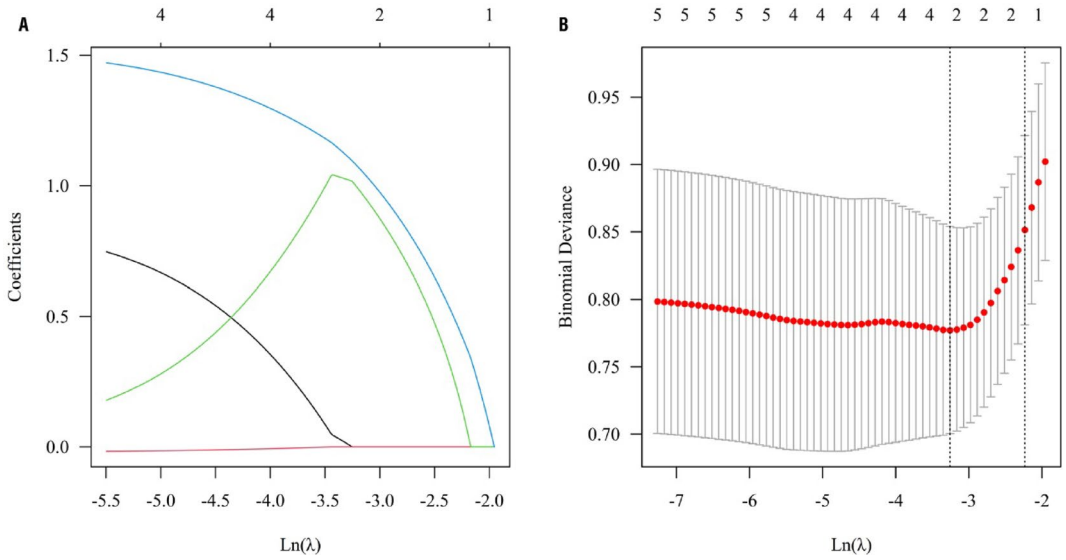

Fig. 2. Feature selected by LASSO regression. (A) Tuning parameters (λ) in the LASSO model used 10-fold cross-validation via minimum criteria. The partial likelihood of deviance was plotted versus log (λ). Dotted vertical lines were drawn at the optimal values using the minimum criteria and the one standard error of the minimum criteria (the 1-SE criteria). (B) Feature coefficients corresponding to different λ values in the LASSO model. A vertical line (optimal λ) was drawn at the value selected using 10-fold cross-validation.

Variables	Odds Ratio (OR)	95% Confidence Interval (CI)	p-value
PSAD	5.296	1.691, 23.972	0.012
SUVmax	4.867	2.389, 10.901	<0.001

Table 2. Multivariate logistic regression analysis for independent predictors in the training set. PV, prostate volume; PSAD, PSA density; SUVmax, maximum standardized uptake value; DRE, digital rectal examination.

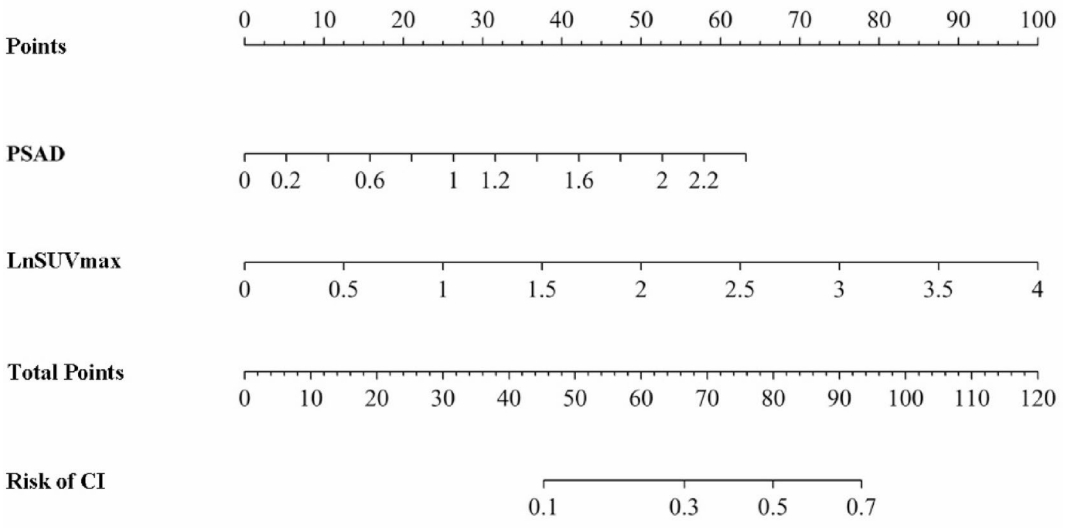

Fig. 3. Nomogram for the csPCa prediction of negative mpMRI. csPCa, clinically significant prostate cancer; PSAD, PSA density.

Diagnostic performance of nomogram

ROC curve analysis was employed to assess the nomogram (Fig. 4). The calibration and clinical application values were evaluated using the calibration curve and DCA (Fig. 4). In the training cohort, the AUC was 0.819, and the calibration curve was close to the ideal diagonal line. Furthermore, the DCA showed significantly better net benefit in the predictive model. The nomogram yielded an AUC of 0.818 (95% CI, 0.719–0.917) and 0.889 (95% CI, 0.832–0.946) in internal and external validation set, respectively (Tabel S5).

The construction of an interactive web risk calculator (PSP Model)

We also designed and published an interactive web risk calculator (www.cspca.online) for convenience. We refer to this PI-RADS/SUVmax/PSAD nomogram model as the PSP Model. After logging into the website, the viewer only needs to input the PI-RADS score, total PSA, three diameters of the prostate (anteroposterior, transverse, and axial diameters), and the SUVmax measured by ^{68}Ga-PSMA PET/CT (Fig. 5). The PSP Model can provide a predicted risk value and prompt whether the patient is high-risk or low-risk for csPCa.

The PSP Model improved the diagnostic performance for negative mpMRI

For detecting csPCa, the PSP Model demonstrated a significant improvement in NPV (93.41% vs. 80.86%) compared with the PI-RADS strategy (Table S6). In addition, the PSP Model also demonstrated a better NRI of 0.8636 (95% CI, 0.5362–1.191) compared to PSAD and 0.3706 (95% CI, 0.0242–0.717) to SUVmax (Table S7). Compared with PSAD and SUVmax, the integrated discrimination improvement (IDI) of the PSP Model was >0 (p<0.05) in different sets (Table S8). Figure 6 displays a typical case in which the PSP Model corrected misdiagnoses in the negative mpMRI.

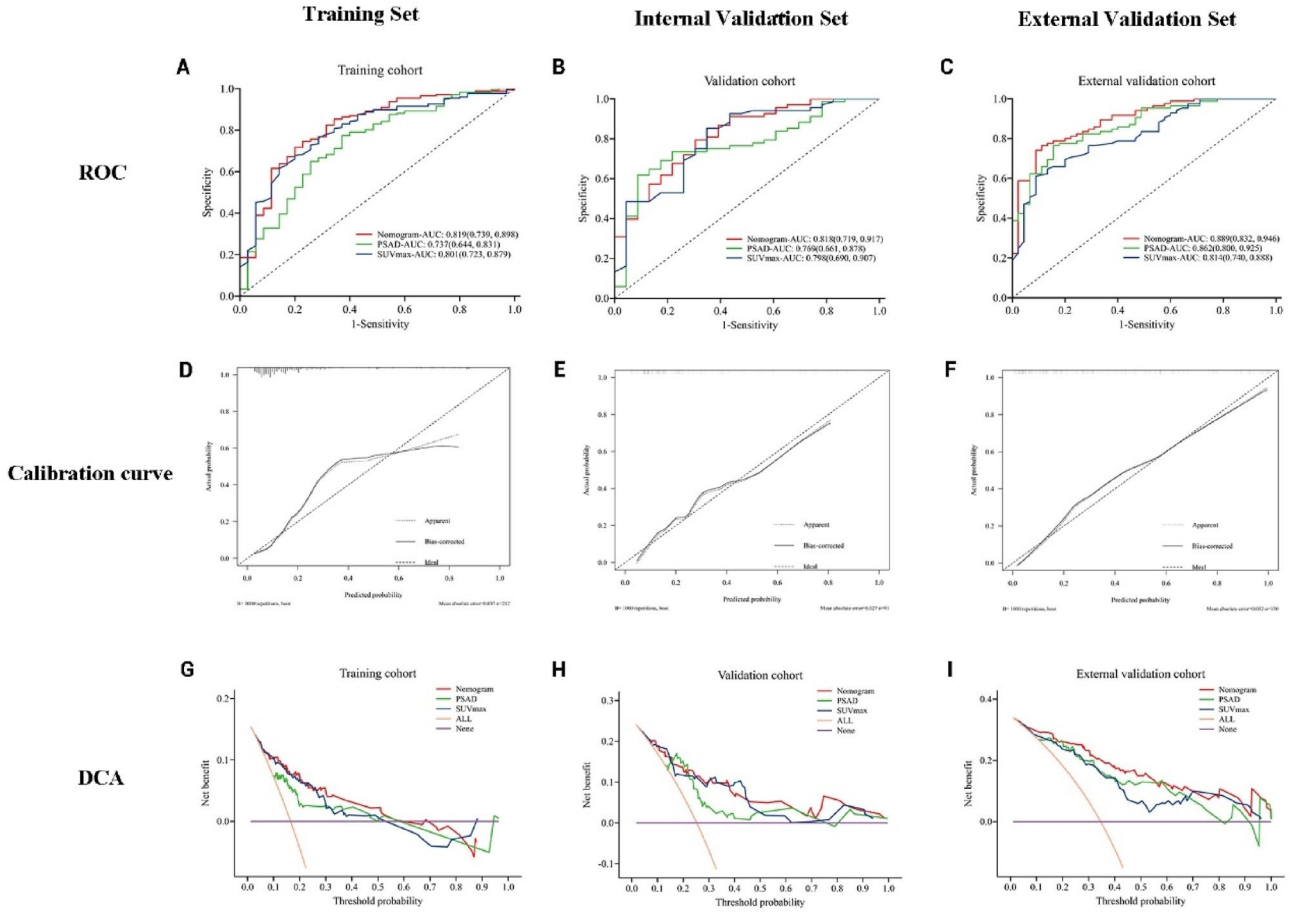

Fig. 4. ROC, calibration curve, and DCA for predicting csPCa across training, internal validation, and external validation sets. ROC, receiver operating characteristic; AUC, area under the ROC curve; DCA, decision curve analysis (A-C) ROC curve in the training set, internal validation set, and external validation set, respectively; (D-F) Calibration curve for predicting the probability of csPCa in negative mpMRI in the training set, internal validation set, and external validation set, respectively; (G-I) Decision curve analysis in prediction of csPCa in negative mpMRI in the training set, internal validation set, and external validation set, respectively.

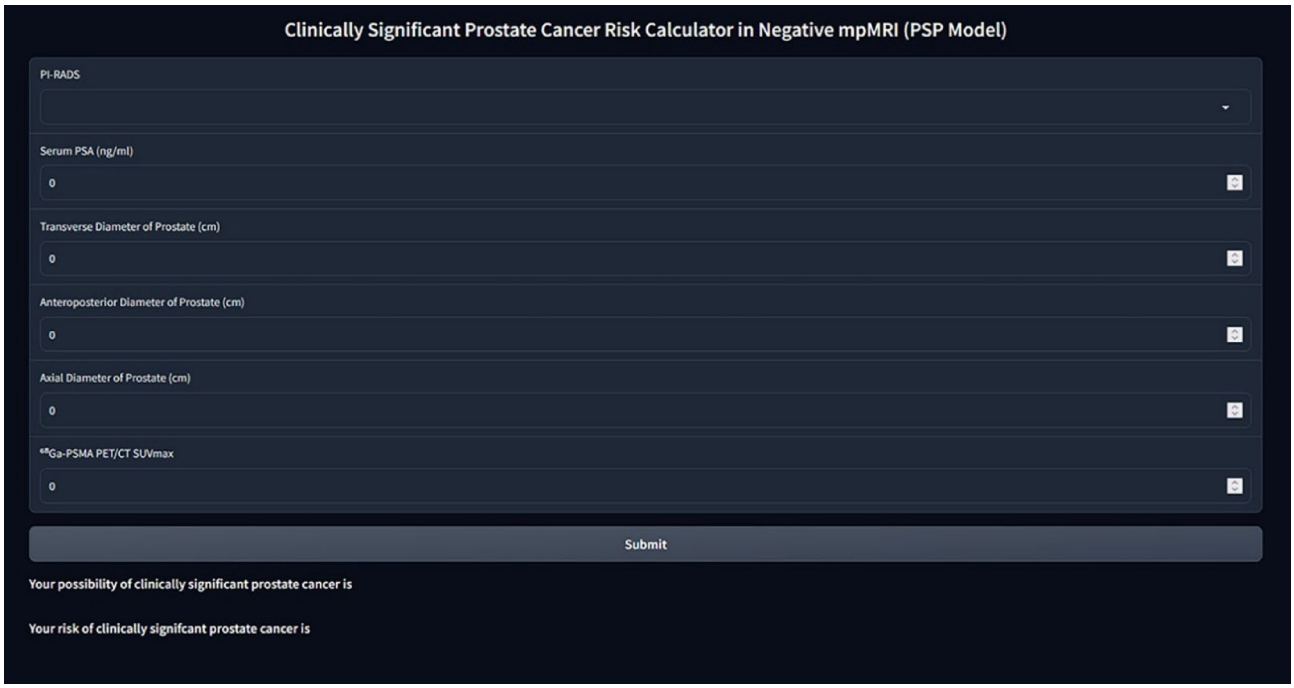

Fig. 5. The web interface of interactive web risk calculator (PSP Model). After the viewers input the PI-RADS score, total PSA, three diameters of the prostate (anteroposterior, transverse, and axial diameters), and the SUVmax of 68Ga-PSMA PET/CT, the PSP Model would provide a predicted risk value and stratification (high- or low- risk) for detecting csPCa in men with negative mpMRI.

Discussion

The use of mpMRI has increased for the localization of newly diagnosed lesions and repeat biopsies due to its sensitivity in detecting csPCa[17]. For positive mpMRI, systematic biopsy plus target biopsy can improve the detection of csPCa. For negative mpMRI, the biopsy can be omitted through shared decision-making with the patient. The proportion of ISUP grade 1–2 lesions on negative mpMRI was the highest[18]consistent with the detection of csPCa by PI-RADS 1–2 in our cohort. However, a negative mpMRI should not be considered enough to omit prostate biopsy owing to the wide variability of mpMRI. The PROMIS study indicated that 27% of men could potentially skip biopsy if mpMRI did not show a suspicious lesion, which could prevent the diagnosis of low-risk prostate cancer in 5%[19]

Our study is the first to develop a nomogram and web-based risk calculator for predicting csPCa in negative mpMRI. The AUC of the PSP Model in predicting csPCa was higher than that of SUVmax (0.819 vs. 0.801) and PSAD (0.819 vs. 0.737). The NRI indicated that the nomogram more accurately reclassified non-csPCa cases into the lower-risk category compared with mpMRI (93.41% vs. 80.86%). Although the NRI of SUVmax was not significant in the internal validation set, IDI shows that it still has an improved predictive effect, but not as significantly as the training set. It has good predictive performance for csPCa in the external validation set. To address the trade-offs between minimizing unnecessary biopsies and reducing missed diagnoses, we did not use the cutoff value of 0.147 based on the maximum Youden index but instead used a cutoff of 0.3 selected based on clinical scenarios. This analysis aims to provide a flexible framework to guide clinical decision-making based on patient-specific or institution-specific priorities[20,21]. This is important to provide reassurance that patients with low PI-RADS scores will not undergo a biopsy.

It is reported that the NPV of mpMRI varies widely, ranging from 69–97%[4]. In our study, the NPV for ruling our csPCa by the nomogram was higher than that of PI-RADS (0.934 vs. 0.809). The EAU Prostate Cancer Guidelines Panel conducted a systematic review of 48 studies with 9,613 patients, aiming to evaluate the promising potential of mpMRI in suspected PCa cases[22]. They reported a median NPV of 88.1% and noted that the NPV varied greatly depending on the definition of positive mpMRI and csPCa. Expanding the definition of a "negative" MRI to include PI-RADS 3 resulted in a decrease in the negative predictive value from 91 to 87%. In addition, despite improvements in mpMRI reporting after introducing the PI-RADS version 2 scoring system, inter-reader variability remains an unsolved problem, particularly when mpMRI is used in centers with little experience. The SWOP calculator (www.prostatecancer-riskcalculator.com) is a nomogram from the European Randomized Study of Screening for Prostate Cancer in predicting the likelihood of a malignant prostate biopsy[23]. SWOP Risk Calculator 4 adds the PI-RADS score of mpMRI to optimize the risk prediction of prostate cancer, especially csPCa. Due to the limitations (age, PV, and PSA limit) of the SWOP calculator, only 84/130 patients in the external validation set were investigated. The results indicated that, in the negative mpMRI group, the PSP model demonstrated a better AUC (0.889 vs. 0.788) and NPV (0.948 vs. 0.768), as is shown in Table S4.

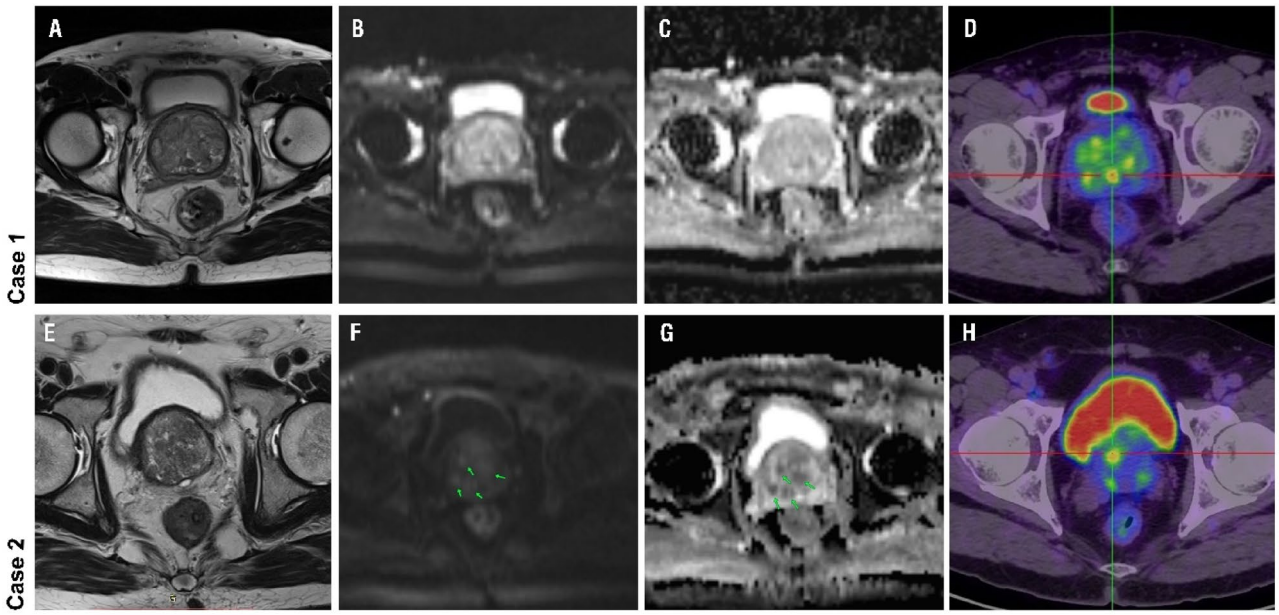

Fig. 6. Correction of misdiagnoses by PSP Model. Case 1. A 72-year-old man with PI-RADS score 2, SUVmax 10.5, PSA 8.4ng/ml, and PSAD 0.40ng/ml/cm3. (A) T2 showed homogeneous hyperplasia of the central and transition zones of the prostate; (B) DWI showed no significant diffusion restriction; (C) ADC signal was not reduced; (D) 68Ga-PSMA PET/CT showed a less obvious focal PSMA activity lesion (crosshair). The PSP Model indicated high risks (33.6% csPCa probability); biopsy pathology was ISUP 2 (Gleason 3+4). Case 2. A 69-year-old man with PI-RADS score 2, SUVmax 10.8, PSA 7.2ng/ml, and PSAD 0.18ng/ml/cm3. (E) T2 showed several well-circumscribed prostate nodules; (F-G) DWI showed slightly diffusion restriction, ADC signal was slightly reduced (green arrow); (H) 68Ga-PSMA PET/CT showed a less obvious focal PSMA activity lesion (crosshair). The PSP Model indicated low risks (27.0% csPCa probability); biopsy pathology were benign prostatic nodules. This figure is only an example case and is not directly representative of the overall statistical performance of the model.

Several studies have shown that ^{68}Ga-PSMA PET/CT can accurately identify csPCa[14,24]. A prospective multicenter phase II imaging trial showed that the strategy SUVmax < 4 (PSMA PET/CT) in negative mpMRI would improve NPV and sensitivity (91% vs. 72%, 97% vs. 83%) for csPCa detecting[24]. Due to the different PSMA ligands and PET/CT cameras used in various centers, there is still a lack of consensus on the quantitative standard (SUVmax) as a reference. Our previous research has shown that the SUVmax cutoff of 5.3 can distinguish csPCa with high sensitivity and specificity[25]. Emmett et al. proposed that the PRIMARY score could optimize the accuracy for csPCa in a low-prevalence population, which is based on a very SUVmax (> 12), the lesion's anatomical location, and intraprostatic PSMA patterns[24]. Our previous study showed that in men with equivocal MRI, negative ^{68}Ga-PSMA PET/CT (PRIMARY score 1–2) + mpMRI (PI-RADS 1–2) could safely avoid unnecessary biopsies[14]. In our study, the PRIMARY score was significantly associated with csPCa in univariate analysis. However, the Logistic multivariate regression identified SUVmax, rather than the PRIMARY score, as a predictor for the nomogram. Additionally, SUVmax is an objective quantitative indicator that is easy to acquire, helping to generalize the model.

PSA density (PSAD) is a well-established predictor of csPCa. When PSAD is used to detect csPCa, the NPV is closely related to the cutoff of PSAD. The EAU guidelines state that for men with negative mpMRI, the risk of finding csPCa at subsequent biopsy is usually ≤ 10% if the PSAD is < 0.15 ng/ml/ml and 27–40% if the PSAD is > 0.15–0.20 ng/ml/ml^2. Deniffel et al. proposed that the PSAD-based MRI model with a cutoff of 0.1 ng/ml can reduce unnecessary biopsies in men with positive MRI at a low-risk threshold (< 5%) and is superior to other existing best-performing MRI models (ERSPC, van Leeuwen, Radtke, and Mehralivand models)[26]. In this study, we observed that the proportion of csPCa in the external validation set (34.6%) was higher than that in the training and internal validation sets. This imbalance in category proportions made it easier for PSAD to differentiate csPCa from non-csPCa (ncsPCa + No Cancer) in the external validation set. Thus, the AUC of PSAD was improved to 0.862. However, this improvement in AUC mainly reflects the impact of the dataset's category distribution on feature performance, rather than enhancing the model's generalization ability. We tried to adjust the class weight, performed a stratified analysis (stratifying by PI-RADS 1/2) strategy, and utilized inverse probability weighting (IPW) to correct for bias. The results indicated an improved detection rate for csPCa, while the discrimination performance for non-csPCa was significantly reduced, resulting in an AUC that was lower than the original model. In the external validation set, the AUC after adjusting class weight, model stratification, and IPW was 0.797, 0.773, and 0.796, respectively. In addition, instead of using a threshold to classify PSAD in the PSP model, we used the raw value as the risk factor.

There are limitations associated with this study. Firstly, given its retrospective design, the study is inherently subject to selection bias. Although both institutions performed strict and normative standards, discrepancies may arise due to the differences in various scanners and parameters that may affect reproducibility. This also reminds us that a larger sample size from multiple centers may be required to validate reproducibility. Second, only two parameters were included in our model. In recent studies, other parameters, such as the ADC value of mpMRI and the radiomics characteristics, have also been diagnostically efficient for csPCa[27]. Finally, although the combination of ^{68}Ga-PSMA PET/CT and mpMRI improves detection rates, the cost increase significantly. Based on the current evidence, we recommend that the following people should be given priority to mpMRI + ^{68}Ga-PSMA PET/CT: ① no suspicious lesions but still present high-risk clinical features, such as PSA ≥ 10 ng/ml or PSAD ≥ 0.15ng/ml/cm^3; ② suspected csPCa despite negative previous biopsy. But these indictions need more research to prove.

Conclusion

In conclusion, this study aimed at the problem that men with negative mpMRI could still be diagnosed with csPCa; we developed and externally validated a nomogram and made an interactive web risk calculator (PSP Model) to identify csPCa and risk stratification in patients with negative mpMRI (PI-RADS 1–2 lesions). The PSP Model has great clinical application and provides a visual and individualized tool for assessing the risk of csPCa in negative mpMRI.

Data availability

Datasets and codes for the study are available from the corresponding author upon reasonable request with a signed agreement for scientific research purposes only.

Received: 19 February 2025; Accepted: 16 July 2025
Published online: 28 July 2025

References

1. Sung, H. et al. Global Cancer statistics 2020: GLOBOCAN estimates of incidence and mortality worldwide for 36 cancers in 185 countries. *Cancer J. Clin.* **71**, 209–249. https://doi.org/10.3322/caac.21660 (2021).
2. Cornford, P. et al. Guidelines on prostate Cancer-2024 update. Part I: screening, diagnosis, and local treatment with curative intent. *Eur. Urol.* **86**, 148–163. https://doi.org/10.1016/j.eururo.2024.03.027 (2024). EAU-EANM-ESTRO-ESUR-ISUP-SIOG.
3. Stephan, C. et al. Interchangeability of measurements of total and free prostate-specific antigen in serum with 5 frequently used assay combinations: An update. *Clin. Chem.***52**, 59–64 (2006).
4. Sathianathen, N. J. et al. Negative predictive value of multiparametric magnetic resonance imaging in the detection of clinically significant prostate cancer in the prostate imaging reporting and data system era: A systematic review and meta-analysis. *Eur. Urol.***78**, 402–414. https://doi.org/10.1016/j.eururo.2020.03.048 (2020).
5. Gan, J. M. et al. Clinically significant prostate cancer detection after a negative prebiopsy MRI examination: Comparison of biparametric versus multiparametric MRI. *AJR Am. J. Roentgenol.***218**, 859–866. https://doi.org/10.2214/ajr.21.26569 (2022).
6. Porpiglia, F. et al. Diagnostic pathway with multiparametric magnetic resonance imaging versus standard pathway: Results from a randomized prospective study in biopsy-naïve patients with suspected prostate cancer. *Eur. Urol.***72**, 282–288. https://doi.org/10.1016/j.eururo.2016.08.041 (2017).
7. Roach, P. J. et al. The impact of 68Ga-PSMA PET/CT on management intent in prostate cancer: results of an Australian prospective multicenter study. *J. Nuclear Medicine: Official Publication Soc. Nuclear Med.* **59**, 82–88. https://doi.org/10.2967/jnumed.117.197160 (2018).
8. Van Damme, J. et al. Comparison of ^{68}Ga-prostate specific membrane antigen (PSMA) positron emission tomography computed tomography (PET-CT) and whole-body magnetic resonance imaging (WB-MRI) with diffusion sequences (DWI) in the staging of advanced prostate cancer. *Cancers***13**, https://doi.org/10.3390/cancers13215286 (2021).
9. Rhee, H. et al. Prostate specific membrane antigen positron emission tomography may improve the diagnostic accuracy of multiparametric magnetic resonance imaging in localized prostate cancer. *J. Urol.***196**, 1261–1267. https://doi.org/10.1016/j.juro.2016.02.3000 (2016).
10. Falkenbach, F. et al. Size and SUVmax define the contribution of nodal metastases to PSA in oligorecurrent prostate cancer. *Prostate***85**, 105–111. https://doi.org/10.1002/pros.24806 (2025).
11. Sonni, I. et al. Head-to-Head comparison of 68Ga-PSMA-11 PET/CT and MpMRI with a histopathology gold standard in the detection, intraprostatic localization, and determination of local extension of primary prostate cancer: results from a prospective Single-Center imaging trial. *J. Nuclear Medicine: Official Publication Soc. Nuclear Med.* **63**, 847–854. https://doi.org/10.2967/jnumed.121.262398 (2022).
12. Turkbey, B. et al. Prostate imaging reporting and data system version 2.1: 2019 update of prostate imaging reporting and data system version 2. *Eur. Urol.***76**, 340–351. https://doi.org/10.1016/j.eururo.2019.02.033 (2019).
13. Zhang, Q. et al. Comparison of 68Ga-PSMA-11 PET-CT with MpMRI for preoperative lymph node staging in patients with intermediate to high-risk prostate cancer. *J. Translational Med.* **15**, 230. https://doi.org/10.1186/s12967-017-1333-2 (2017).
14. Guo, S. et al. The PRIMARY score: Diagnostic performance and added value compared with MRI in detecting clinically significant prostate cancer. *Clin. Nucl. Med.***49**, 37–44. https://doi.org/10.1097/rlu.0000000000004951 (2024).
15. Offermann, A., Hupe, M. C., Sailer, V., Merseburger, A. S. & Perner, S. The new ISUP 2014/WHO 2016 prostate cancer grade group system: First résumé 5 years after introduction and systemic review of the literature. *World J. Urol.***38**, 657–662. https://doi.org/10.1007/s00345-019-02744-4 (2020).
16. Schaeffer, E. M. et al. Prostate cancer, version 4.2023, NCCN clinical practice guidelines in oncology. *J. Natl. Compr. Cancer Network: JNCCN.* **21**, 1067–1096. https://doi.org/10.6004/jnccn.2023.0050 (2023).
17. Rouvière, O. et al. Use of prostate systematic and targeted biopsy on the basis of multiparametric MRI in biopsy-naive patients (MRI-FIRST): A prospective, multicentre, paired diagnostic study. *Lancet Oncol.***20**, 100–109. https://doi.org/10.1016/s1470-2045(18)30569-2 (2019).
18. Yaxley, W. J. et al. Histological findings of totally embedded robot assisted laparoscopic radical prostatectomy (RALP) specimens in 1197 men with a negative (low risk) preoperative multiparametric magnetic resonance imaging (mpMRI) prostate lobe and clinical implications. *Prostate Cancer Prostatic Dis.* **24**, 398–405. https://doi.org/10.1038/s41391-020-00289-x (2021).
19. Ahmed, H. U. et al. Diagnostic accuracy of multi-parametric MRI and TRUS biopsy in prostate cancer (PROMIS): a paired validating confirmatory study. *Lancet (London England).* **389**, 815–822. https://doi.org/10.1016/s0140-6736(16)32401-1 (2017).

20. Rieger, T. R. et al. Improving the generation and selection of virtual populations in quantitative systems pharmacology models. *Prog. Biophys. Mol. Biol.***139**, 15–22. https://doi.org/10.1016/j.pbiomolbio.2018.06.002 (2018).
21. Clark, L. et al. A methodological review of recent meta-analyses has found significant heterogeneity in age between randomized groups. *J. Clin. Epidemiol.***67**, 1016–1024. https://doi.org/10.1016/j.jclinepi.2014.04.007 (2014).
22. Moldovan, P. C. et al. What is the negative predictive value of multiparametric magnetic resonance imaging in excluding prostate cancer at biopsy?? A systematic review and meta-analysis from the European association of urology prostate cancer guidelines panel. *Eur. Urol.***72**, 250–266. https://doi.org/10.1016/j.eururo.2017.02.026 (2017).
23. Birch, A., Withington, J., Kinsella, J., Acher, P. & Challacombe, B. Use of the SWOP calculator to reduce unnecessary prostate biopsies in men with elevated PSA. *Int. J. Surg.* **10** https://doi.org/10.1016/j.ijsu.2012.06.513 (2012).
24. Emmett, L. et al. The additive diagnostic value of prostate-specific membrane antigen positron emission tomography computed tomography to multiparametric magnetic resonance imaging triage in the diagnosis of prostate cancer (PRIMARY): A prospective multicentre study. *Eur. Urol.***80**, 682–689. https://doi.org/10.1016/j.eururo.2021.08.002 (2021).
25. Jiao, J. et al. Establishment and prospective validation of an SUVmax cutoff value to discriminate clinically significant prostate cancer from benign prostate diseases in patients with suspected prostate cancer by 68Ga-PSMA PET/CT: A real-world study. *Theranostics***11**, 8396–8411. https://doi.org/10.7150/thno.58140 (2021).
26. Deniffel, D. et al. Avoiding unnecessary biopsy: MRI-based risk models versus a PI-RADS and PSA density strategy for clinically significant prostate cancer. *Radiology***300**, 369–379. https://doi.org/10.1148/radiol.2021204112 (2021).
27. Woźnicki, P. et al. Multiparametric MRI for prostate Cancer characterization: combined use of radiomics model with PI-RADS and clinical parameters. *Cancers* **12** https://doi.org/10.3390/cancers12071767 (2020).

Author contributions

HW, GSK and MXL contributed to the conceptualization and design of the study. MSJ, YL, ZLL, CJ, WFL and HHZ collected the data. WJY, KF, WY and RJ were responsible for the PRIMARY and PI-RADS scoring. ZC, JYM, ZKY and LY conducted the analysis. HW led the writing of the original draft. HDH, and ZKY edited the manuscript, discussed results, and provided feedback regarding the manuscript. QWJ and ZJL supervised the study and acquired funding. QWJ, GHQ and RJ supervised and managed the entire project. All authors had full access to the data and approved the manuscript for publication.

Funding

This work was supported by the National Natural Science Foundation of China (82302244 and 82220108004), the Medical Scientific Research Projects of Dalian (20Z12019 and 2112018), and the Clinical and Basic Medicine Innovation Research Project of Xijing Hospital (LHJJ24JH244). No other potential conflict of interest relevant to this article was reported.

Declarations

Competing interests

The authors declare no competing interests.

Ethical approval and contest to participate

This retrospective study was approved by the Medical Ethics Committee of Xijing Hospital (KY20242255-F-3) and the Ethics Committee of Medical Nanjing Drum Tower Hospital (2024-0002-07). Both ethics committees waived the requirement for informed consent due to the anonymized and retrospective nature of the study. All methods were carried out in accordance with relevant guidelines and regulations.

Additional information

Supplementary Information The online version contains supplementary material available at https://doi.org/10.1038/s41598-025-12312-z.

Correspondence and requests for materials should be addressed to W.Q.